ELSEVIER

Journal of Alloys and Compounds 293–295 (1999) 156–160

Journal of
ALLOYS
AND COMPOUNDS

Phase composition and the effect of thermal cycling for VH$_x$, V$_{0.995}$C$_{0.005}$H$_x$, and V$_{0.975}$Zr$_{0.020}$C$_{0.005}$H$_x$

J.S. Cantrell[a],*, R.C. Bowman Jr.[b]

[a]Department of Chemistry and Biochemistry, Miami University, Oxford, OH 45056, USA
[b]Jet Propulsion Laboratory, California Institute of Technology, 4800 Oak Grove Drive, Pasadena, CA 91109, USA

Abstract

X-ray diffraction (XRD) studies were performed on hydride phases formed by vanadium and its carbon substituted alloys. It was previously found that thermal cycling of VH$_x$ across the β–γ mixed phase region changed the reversible hydrogen storage capacity and other properties. The present materials were compared where annealing was one prior treatment and the materials were cycled from 3 cycles to over 1000 cycles and one sample was cycled 6182 times. The effects on phase composition, c/a unit cell axial ratios, unit cell volume and crystallite particle size and BET surface area measurements were studied. Earlier studies placed the β–γ phase boundary at $x = 0.82$ for XRD studies. The phase boundaries of the substituted alloys are found to be virtually the same. Thermal cycling produced similar behavior for all the materials. © 1999 Elsevier Science S.A. All rights reserved.

Keywords: Vanadium alloys; Vanadium hydride; X-ray diffraction; Pressure-composition-temperature isotherms; Scanning electron microscopy

1. Introduction

The hydrides of vanadium and its carbon substituted alloys have been investigated for hydrogen compressors and other applications [1–3]. Previous XRD studies have resulted in determining the β–γ boundary for the VH$_x$ phases [4]. The pressure range and reversible hydrogen storage capacity for the mixed phase region between the nominal monohydride (β) and dihydride (γ) VH$_x$ phases [5,6] are very attractive for various applications including closed-cycle cryogenic refrigerators [7]. The hydride beds may involve 10^4–10^5 absorption–desorption reactions in an application. Although the VH$_x$, V–C–H$_x$, and V–Zr–C–H$_x$ systems cannot experience the intrinsic chemical disproportionation reactions that occur [8] in LaNi$_5$H$_x$ and other ternary hydrides, we have observed changes in the isotherms for VH$_x$, V$_{0.995}$C$_{0.005}$H$_x$, and V$_{0.995}$Zr$_{0.020}$C$_{0.005}$H$_x$ after several hundred absorption–desorption cycles across the β–γ plateau region. In addition, these thermally cycled hydrides produced a low-density material that caused swelling or even rupture of the reaction vessels [9]. This paper summarizes changes in the compounds studied for the isotherms for the β–γ plateau,

XRD studies, surface area, strain and other properties of the materials changed by the thermal cycling treatments.

2. Experimental procedures

These studies used high purity vanadium metal that had been processed by the United States Bureau of Mines. A sample consisting of a 4.9 g button was sealed under vacuum and annealed at 1470 K for 40 h. After an initial activation treatment involving 10 hydrogen reaction cycles, the absorption–desorption isotherms across the β–γ region was measured at 298 K. The reactor was operated [10] by thermal cycling with ultrapure hydrogen gas by heating the reactor between 297 and 408 K with a nominal 1 h repeat period. During the initial cycles the pressure varied between 11.8 and 14.1 bar. This pressure increase indicated that the hydride composition changed across the entire β–γ mixed phase region for the approximate 0.5 L volume of the cycling apparatus. After a sample had been cycled 1000 times, the isotherms at 298 K were measured again [3]. A second sample was hydrogen activated after a 24 h anneal at 1473 K and taken through 11 absorption–desorption cycles [3].

The vanadium–carbon alloys were prepared by arc-melting to form buttons. Since powders are difficult to

*Corresponding author. Tel.: +1-513-529-2813; fax: +1-513-529-5715.

0925-8388/99/$ – see front matter © 1999 Elsevier Science S.A. All rights reserved.
PII: S0925-8388(99)00386-2

produce from the arc-melted vanadium alloy buttons, filings were obtained using a milling machine, which caused extensive cold working [9,11]. The filings were annealed at 1470 K to reduce the effects of this cold-working on the hydrogen absorption properties of the alloys. The $V_{0.995}C_{0.005}$ alloy was cycled between 296 and 444 K under similar conditions to those used on the pure V samples. The pressure swings during the temperature cycles were initially between 12.1 and 14.0 bar which produced complete transitions across the β–γ two-phase region.

The alloy $V_{0.975}Zr_{0.020}C_{0.005}$ was placed in a different system [9] where it was subjected to more rapid cycling between 291 and 367 K with 10 min periods for the heating–cooling cycles. The zirconium had been added to this alloy to facilitate activation under the conditions used for this thermal cycling series [9]. The pressure changes were initially between 10.1 and 12.1 bar during cycling which indicated approximately 70% conversion between the β and γ phases for the $V_{0.975}Zr_{0.020}C_{0.005}$ sample while 100% transformations had been obtained from the V and $V_{0.995}C_{0.005}$ samples.

The physical and structural properties of the powders after the 11, 1000, and 6182 thermal cycles were characterized by XRD, surface areas analysis using the well-known [12] Brunauer–Emmett–Teller (BET) method, and scanning electron microscopy (SEM) studies of the morphology for these materials.

3. Results and discussion

Experimental isotherms for the VH_x sample have been previously reported [3]. The 298 K absorption and desorption isotherms for $V_{0.995}C_{0.005}H_x$ and $V_{0.995}Zr_{0.020}C_{0.005}H_x$ are presented in Figs. 1 and 2, respectively. The hysteresis ratio of the absorption–desorption isotherms for VH_x increased from 1.8 to 2.7 after 1000 cycles due to the greater absorption pressures that were accompanied by a 20% decrease in the effective absorption storage capacity (Δx_{abs}). This behavior does not correspond to the degradation observed when AB_5 hydrides were cycled [8,10] and its origins cannot be attributed to alloy segregation. Furthermore, the high purity of the research grade hydrogen gas as well as the various precautions taken to avoid leaks or other sources of contamination should minimize any stoichiometry loss due to oxidation processes.

The parameters presented in Table 1 summarize the hydriding properties of the vanadium–carbon alloys. Carbon has little impact on Δx_{abs} after activation or after thermal cycling which produces about a 20% loss, while the initial hysteresis ratio P_f/P_d is smaller for the $V_{0.995}C_{0.005}$ alloy compared to pure vanadium, the ratio is larger after cycling. However, these differences are probably within the experimental uncertainties for the isotherms. The Zr alloying apparently increases the initial hysteresis
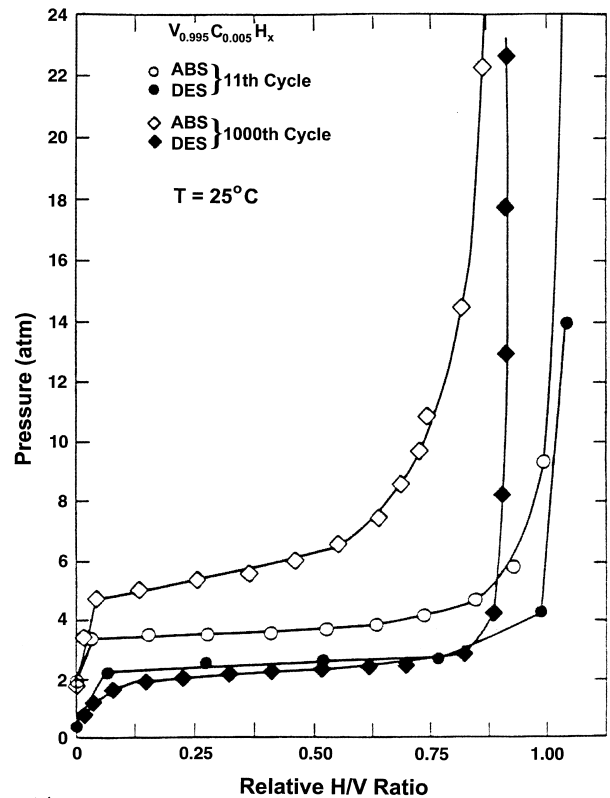

Fig. 1. Reversible portions of the pressure–composition isotherms obtained at 298 K on thermal cycled $V_{0.995}C_{0.005}H_x$.

but gives a value between the other materials after cycling. As has been observed previously [3], thermal cycling produces a large increase in the powder surface areas for the three alloys. In fact, carbon appears to enhance the
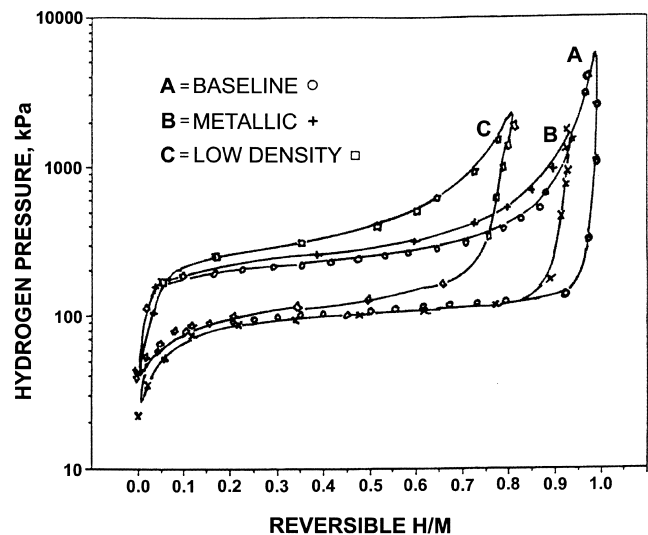

Fig. 2. Reversible portions of the pressure–composition isotherms obtained at 298 K on thermal cycled $V_{0.975}Zr_{0.020}C_{0.005}H_x$. The curves labeled A were obtained after 11 cycles while the curves B (fractured metallic portion) and C (sponge-like, black, low-density material) were measured after 6182 cycles between 291 and 367 K.

Table 1
Impact of thermal cycling on some properties of hydride phase of vanadium–carbon alloys

Composition of cycled material	Phases found	Number of cycles	P_r/P_d	Δx_{abs}	Surface area (m^2/g)
$VH_{0.83}$	$\beta + \gamma$	11	1.8	1.04	0.35
$VH_{1.39}$	$\gamma + \beta$	1000	2.7	0.78	15.5
$V_{0.995}C_{0.005}H_{0.78}$	β	11	1.45	1.00	0.86
$V_{0.995}C_{0.005}H_{0.40}$	β	1000	3.2	0.81	38.2
$V_{0.975}Zr_{0.02}C_{0.005}H_{0.82}$	$\beta + \gamma$	11	2.4	0.95	N/A
$V_{0.975}Zr_{0.02}C_{0.005}H_{0.44}$	β	6182	2.9	0.74	5.4

surface area during both activation and cycling. The relatively low surface area of 5.4 m²/g for the $V_{0.975}Zr_{0.020}C_{0.005}$ sample after 6182 cycles is due to the presence of two morphologies arising from partial conversion between the β and γ phases during cycling.

Table 2 summarizes the materials studied, the treatment of the samples, number of cycles, the H/M or x value for samples after cycling as determined by the quantitative desorption method [4], the phases identified by XRD, and the particle size from XRD line broadening using both the Warren–Averback and extrapolation methods [3]. Although published V–H phase diagrams [13,14] indicate other phases (i.e., ε and η) besides the β-phase over the composition range $0.5 < x < 1.0$, these phases are simple variants of the body-centered tetragonal (bct) β–V_2H structure arising from either ordering or disordering of additional hydrogen on the octahedral interstitial sites [13,14]. Powder XRD cannot easily distinguish between the β, ε, and η phases [4]; hence, the β-phase is used here to denote the nominal monohydride bct phase. The upper concentration limit for β-phase at room temperature was previously shown [4] to be $VH_{0.82}$ and the carbon substitution has negligible impact on this phase boundary. A

number of the samples contained both γ and β phases. Particle size does not correlate with the number of cycles although the longest number of cycles does appear to correspond to a smaller particle size. The unit cell parameters and lattice volumes indicate that the crystal lattice does not change much with cycling — even for the 6182 cycles of the $V_{0.975}Zr_{0.020}C_{0.005}H_x$ sample.

Previously reported scanning electron micrographs [3] for VH_x, that compared typical sample particles from different cycling conditions, showed significant changes in morphology. After 11 hydriding–dehydriding cycles, the VH_x particles have sharp irregular features with numerous cracks and fissures. However, 1000 cycles lead to highly textured particles with much internal void space to give a sponge-like appearance. This effect is supported by the substantial increase in the BET surface areas from 0.35 ± 0.07 m²/g to 15.5 ± 0.5 m²/g after 1000 cycles. The SEM images obtained from the $V_{0.995}C_{0.005}H_x$, material before and after the extended cycling looked identical to those for the corresponding VH_x samples. The SEM micrographs for the activated $V_{0.975}Zr_{0.020}C_{0.005}H_x$ material revealed very similar highly fractured particles as shown in Fig. 3(a,b). However, a much more complex morphology was found for $V_{0.975}Zr_{0.020}C_{0.005}H_x$ after the 6182 rapid cycles, which is illustrated in Fig. 3(c,d). A significant quantity of irregularly fractured pieces are present in addition to the majority sponge-like particles similar to those seen for cycled VH_x and $V_{0.995}C_{0.005}H_x$. This difference can be attributed to the incomplete conversion of a fraction of the $V_{0.975}Zr_{0.020}C_{0.005}H_x$ particles during the rapid cycling over a reduced temperature change. Hence, a fraction of the particles retain their initial activated shapes and hydrogen absorption properties.

Although $LaNi_5$ and many other intermetallic hydrogen

Table 2
Phase composition and lattice parameters from powder XRD for cycled VH_x, $V_{0.995}C_{0.005}H_x$, and $V_{0.975}Zr_{0.020}C_{0.005}H_x$

Sample composition[a]	Initial alloy annealing treatment	Number thermal cycles	Phases identified by XRD	a_o (nm)	c_o (nm)	c/a ratio	Volume $(10^{-2}\ nm^3)$	Particle size from XRD peak widths (nm)
V	Unannealed	0	α (bcc)	0.30279(13)	–	–	2.776(4)	N/A
$VH_{0.83}$	1473 K/24 h	11	β (bct)	0.3027(1)	0.3394(2)	1.1213	3.109(2)	25.2
			γ (fcc)	0.4265(6)	–	–	7.76(4)	29.1
$VH_{1.39}$	1473 K/40 h	1000	β (bct)	0.3026(2)	0.3432(5)	1.1342	3.143(5)	19.6
			γ (fcc)	0.4275(3)	–	–	7.813 (11)	25.0
$V_{0.995}C_{0.005}$	1473 K/24 h	0	α (bcc)	0.30313(9)	–	–	2.785(3)	N/A
$V_{0.995}C_{0.005}H_{0.83}$	Unannealed filings	11	β (bct)	0.3023(1)	0.3395(1)	1.1231	3.103(1)	17.7
$V_{0.995}C_{0.005}H_{0.78}$	1473 K/24 h	11	β (bct)	0.3019(1)	0.3405(1)	1.1279	3.103(1)	25.2
$V_{0.995}C_{0.005}H_{0.40}$	1473 K/24 h	1000	β (bct)	0.3011(1)	0.3340(1)	1.1093	3.0275(8)	17.7
$V_{0.975}Zr_{0.020}C_{0.005}$	1473 K/24 h	0	α (bcc)	0.30315(7)	–	–	2.786(2)	N/A
$V_{0.975}Zr_{0.020}C_{0.005}H_{0.82}$	Unannealed milled chips	11	β (bct)	0.3033(3)	0.3424(4)	1.1289	3.150(7)	22.1
			γ (fcc)	0.4278(3)			7.829(7)	25.0
$V_{0.975}Zr_{0.020}C_{0.005}H_{0.44}$	Unannealed milled chips	6182	β (bct)	0.3038(3)	0.3348(7)	1.1020	3.090(6)	14.7

[a] Compositions for these hydride samples were determined by desorption method from Ref. [4] after completion of the number of hydrogen absorption desorption cycles indicated.
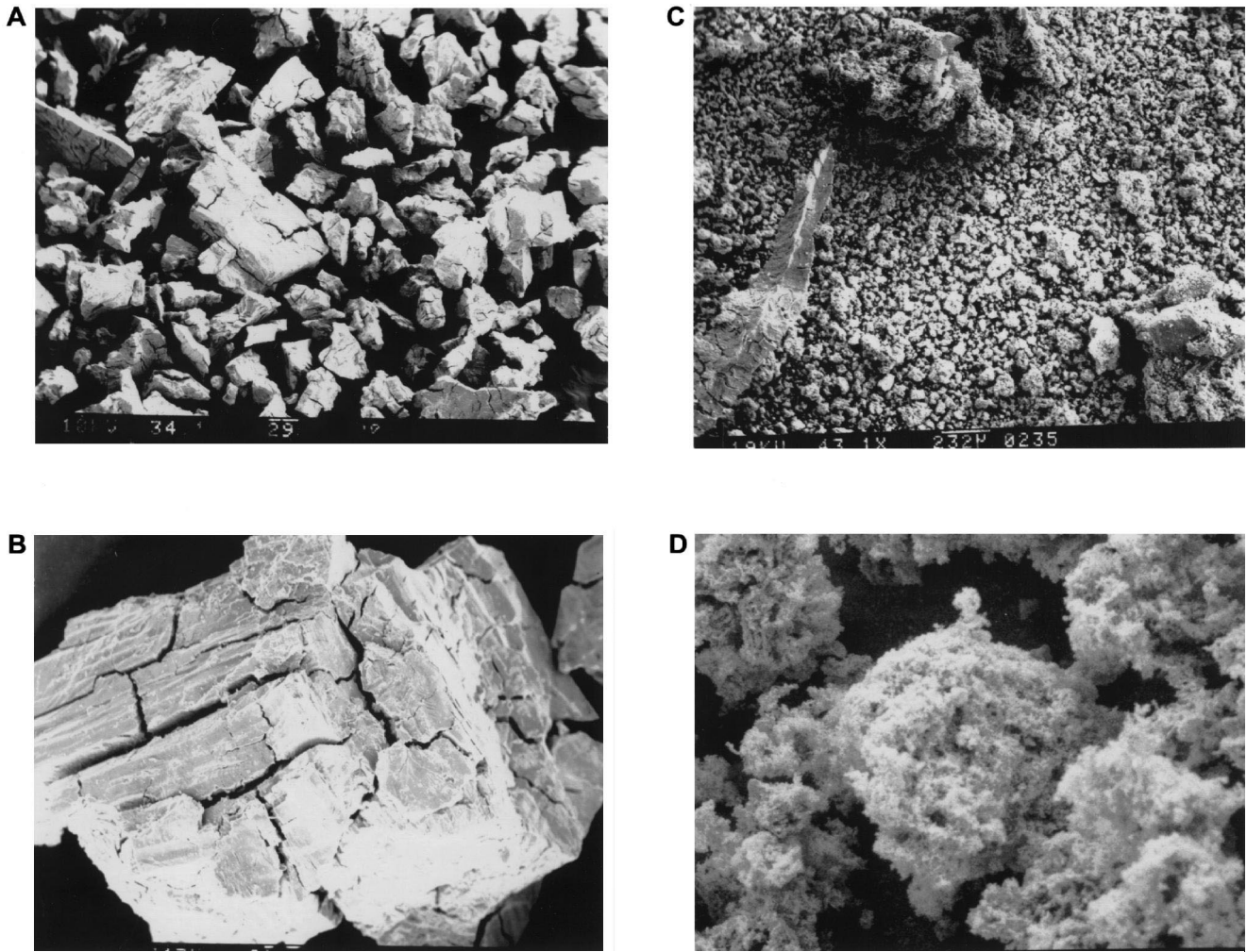
Fig. 3. Scanning electron micrographs of representative $V_{0.975}Zr_{0.020}C_{0.005}H_x$ particles after cycling between 291 and 367 K for 11 cycles in (a) and (b) and for 6182 cycles in (c) and (d).

storage systems will become fine powders after several hydriding cycles, these particles usually retain the morphology created during the activation treatment with rather modest additional increases in surface area (i.e., less than 10-fold larger) unless contamination processes were also occurring [15]. However, $LaNi_5$ related alloys are much more brittle than vanadium and have a propensity towards intergranular and transgranular fracture upon hydrogenation [16]. In contrast, decrepitation of V-containing samples appears to occur via a ductile fracture process [16], which leads to a distinctive morphology that appears to be like a sponge with many open spaces and a reduced density.

Thermal cycling also leads to major changes in the microstructures of the various hydrides of V-containing particles, which are evident from transmission electron microscopy studies [3]. The hydride particles of V, $V_{0.995}C_{0.005}$, and $V_{0.995}Zr_{0.020}C_{0.005}$ after ~10 cycles were found to have large populations of individual domains with dimensions between 4 and 5 nm and had spotty powder

diffraction rings from the selected area electron diffraction. The images obtained from material particles that had undergone 1000 cycles consisted mostly of domains that are 15 nm or larger (compared to 5 nm domains at 10 cycles). In addition, distinct spot patterns are observed from these larger (15 nm) regions [3]. There was some variation of the domain sizes (4–20 nm) after ~1000 cycles which indicates that this process may be complex. The increase in absorption pressure after 1000 cycles does correlate with an increase in domain size. The broadening of XRD peaks in similarly cycled $V_{0.995}C_{0.005}H_x$ samples [17] indicated a two-fold increase in domain size and a 40% decrease in lattice strain after 778 thermal cycles. Decreases in lattice strain have been correlated [18] with increased absorption pressure in $LaNi_5H_x$. The fact that lattice strain and domain dimensions may significantly influence hydrogen absorption behavior for VH_x, $V_{0.995}C_{0.005}H_x$, and $V_{0.995}Zr_{0.020}C_{0.005}H_x$ in these thermal cycling experiments is probably related to the cold-working process [11,17] during the incorporation and release of

the hydrogen. This change may be an effect similar to annealing because of the stretching and compressing of the lattice metal atoms. Additional studies of these and other related materials that have undergone thermally H-absorption/desorption cycles must be carried out to determine in greater detail the actual mechanisms.

Acknowledgements

References

[1] R.C. Bowman Jr., B.D. Freeman, E.L. Ryba, R.E. Spjut, E.A. Liu, J.M. Penso, F.E. Lynch, Z. Phys. Chem. 183 (1994) 245.

[2] B.D. Freeman, E.L. Ryba, R.C. Bowman Jr., J.R. Phillips, Int. J. Hydrogen Energy 22 (1997) 1125.

[3] R.C. Bowman Jr., F.E. Lynch, R.W. Marmaro, C.H. Luo, B. Fultz, J.S. Cantrell, D. Chandra, Z. Phys. Chem. 181 (1993) 269.

[4] J.S. Cantrell, R.C. Bowman Jr., A. Attalla, R.W. Baker, Z. Phys. Chem. 181 (1993) 83.

[5] J.J. Reilly, R.H. Wiswall Jr., Inorg. Chem. 9 (1970) 1678.

[6] W. Luo, J.D. Clewley, T.B. Flanagan, J. Chem. Phys. 93 (1990) 6710.

[7] R.C. Bowman Jr., B.D. Freeman, J.R. Phillips, Cryogenics 32 (1992) 127.

[8] H.-J. Ahn, J.-Y. Lee, Int. J. Hydrogen Energy 16 (1991) 93.

[9] R.W. Marmaro, F.E. Lynch, D. Chandra, Investigation of Long Term Stability in Metal Hydrides, NAS9-18175 by HCI, 12410 North Dumont Way, Littletown, CO 80125 November, 1991.

[10] S.W. Lambert, D. Chandra, W.N. Cathey, F.E. Lynch, R.C. Bowman Jr., J. Alloy Comp. 181 (1992) 113.

[11] T.B. Flanagan, H. Noh, J.D. Clewley, R.C. Bowman Jr., Scripta Met. 28 (1993) 355.

[12] S. Lowell, J.E. Shields, Powder Surface Area and Porosity, Chapman and Hall, London, 1984.

[13] J.F. Smith, D.T. Peterson, in: J.F. Smith (Ed.), Phase Diagrams of Binary Vanadium Alloys, ASM International, Metals Park, OH, 1989, p. 106.

[14] T. Schober, Solid State Phenomena 49–50 (1996) 357.

[15] J.J.G. Willems, Philips J. Res. 39 (Suppl. 1) (1984) 1.

[16] I.R. Harris, P.J. McGuiness, J. Less-Common Met. 172–174 (1991) 1273.

[17] A. Sharma, M.S. Thesis, Department of Physics, University of Nevada-Reno, 1992.

[18] K. Nomura, H. Uruno, S. Ono, H. Shinozuka, S. Suda, J. Less-Common Met. 107 (1985) 221.